VIP Surface-Enhanced Spectroscopy

DOI: 10.1002/anie.201204973

Gold Nanoparticle Capping Layers: Structure, Dynamics, and Surface Enhancement Measured Using 2D-IR Spectroscopy**

*Paul M. Donaldson and Peter Hamm**

Raman and infrared spectroscopic analysis play an important practical role in nanotechnology research. From surface-assembled monolayer characterization[1a,b] to sensing[2] and labeling,[3] the vibrational bands in Raman and infrared spectra are useful for identifying the presence of specific molecules in a sample and reporting on their structure, charge state, orientation, and local solvation.

As a recent development, more advanced methods of ultrafast multidimensional infrared spectroscopy[4a,b,c,d] are increasingly used for measurements where detailed spectroscopic information about the molecular structure, dynamics, and environment is required, or where an infrared or Raman spectrum is too congested for straightforward analysis. One such technique, two-dimensional infrared spectroscopy (2D-IR), employs a sequence of short infrared laser pulses that excite selected vibrational states of a molecular system.[5a,b] The evolution of the excited vibrational states and depleted ground state is time resolved over a range of about 10^{-13}–10^{-10} s using a delayed probe pulse.

2D-IR spectra contain information unobtainable in linear spectra. The shape of the diagonal peaks in a 2D spectrum are a powerful probe of structural dynamics[6a,b] and cross peaks appear through direct vibrational couplings,[7a,b] population relaxation,[8] and chemical exchange.[9a,b] Measurements on surface-assembled monolayers[10a,b] and nanoparticle capping layers[11] indicate that 2D-IR spectroscopy can contribute significantly to the characterization of nanostructured systems. We will show in this paper that 2D-IR spectroscopy is especially sensitive to the changes in local environment and dynamics that occur for nanoparticle-bound molecules compared with equivalent unbound molecules.

The additional possibility of localized intensification of electric fields adds another twist to the spectroscopy of metal nanostructures, giving rise to a variety of effects, most notably surface-enhanced Raman scattering[12a,b] (SERS) and surface-enhanced infrared absorption (SEIRA).[13a,b,c,d] Focussing on liquid suspensions of spherical gold nanoparticles and their aggregates, we explore herein how 2D-IR spectroscopy can be applied to the study of molecular adsorbate capping layers in the presence of infrared near-field surface enhancements.

We begin our discussion with a description of how field enhancement, orientational averaging, and local structure effects determine 2D-IR signals from assemblies of molecules around spherical noble metal nanoparticles. Mie theory[14] describes the electric field around a sphere illuminated by an incident field of amplitude E_0. When the nanoparticle radius a is much smaller than the wavelength of the incident light λ, a simplified quasistatic description is obtained[15] (for details, see the Supporting Information). The electric field magnitude in this limit is plotted in Figure 1a. In the infrared, far from the d-sp plasmon resonance, the field has a peak value of $3E_0$ at the nanoparticle surface along the polarization axis. In addition to this increase in field strength, two other effects work together to increase the coupling of the field to the bound molecules. These are the conversion of the polarized incident field into a radial near-field around the nanoparticle and the translation of a random isotropic molecular dipole distribution, as occurs in solution, to a nanoparticle-based surface distribution (Figure 1c and d).

Consider a ground to first excited-state infrared transition ($v=0\rightarrow1$). The infrared absorption A and the 2D-IR signal strength S depend on the field-transition dipole interaction as $\left\langle(\vec{\mu}.\vec{E})^2\right\rangle$ and $\left\langle(\vec{\mu}.\vec{E})^4\right\rangle$, respectively.[4d] The angle brackets $\langle.\rangle$

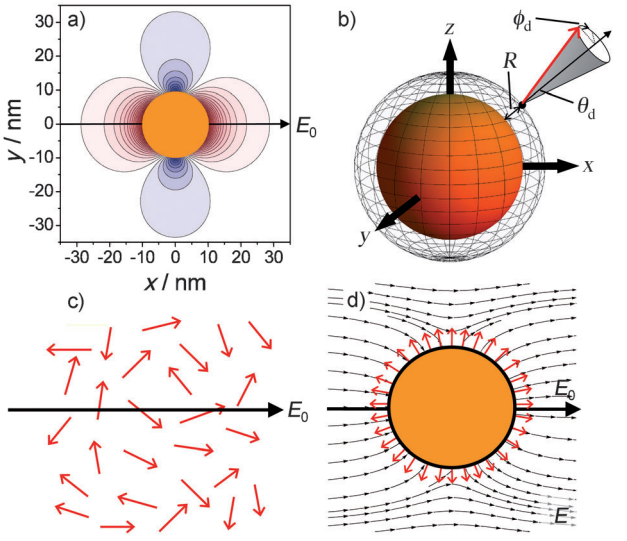

Figure 1. a) The electric field magnitude $|E|$ around a metal nanoparticle under IR illumination. Red describes regions where $|E|>E_0$. Blue describes regions where $|E|<E_0$. b) Coordinates used to describe nanoparticle-bound transition dipoles. c) An isotropic distribution of transition dipoles in an *x*-polarized electric field. d) A radial distribution of transition dipoles in a metal nanoparticle near field.

[*] P. M. Donaldson, P. Hamm
Institute of Physical Chemistry, University of Zürich
Winterthurerstrasse 190, 8057 Zürich (Switzerland)
E-mail: phamm@pci.uzh.ch

[**] The authors are grateful to Jan Helbing and Thomas Feurer for helpful discussions, and Shabir Hassan for assistance with the TEM characterization of the nanoparticles. This work was supported by an advanced ERC investigator grant (DYNALLO) to P.H. and by the Swiss National Science Foundation through the NCCR network "MUST".

Supporting information for this article is available on the WWW under http://dx.doi.org/10.1002/anie.201204973.

indicate averaging over the orientations of a dipole of strength μ_0 with respect to the field. For an isotropic distribution of vibrational transition dipoles, we have for absorption A and diagonal 2D-IR signal S the well-known Equations (1) and (2):[4d]

$$A^{IR}_{isotropic} \propto \mu_0^2 E_0^2/3 \quad (1)$$

$$S^{2D-IR}_{isotropic} \propto \mu_0^4 E_0^4/5 \quad (2)$$

For an array of transition dipoles on a metal nanosphere surface oriented radially outwards (Figure 1 d), the field is always aligned with the molecular dipoles. At the surface, the radial field is $3E_0 \sin\theta\cos\phi$ (see the Supporting Information). Averaging over θ and ϕ gives Equations (3) and (4):

$$A^{\mathrm{IR}}_{\mathrm{nanoparticle}} \propto 3\mu_0^2 E_0^2 \quad (3)$$

$$S^{\mathrm{2D-IR}}_{\mathrm{nanoparticle}} \propto 81\mu_0^4 E_0^4/5 \quad (4)$$

Using the isotropic case for reference, we define the following signal and absorption enhancement factors [Eqs. (5) and (6)]:

$$Q_{\mathrm{2D-IR}} = S^{\mathrm{2D-IR}}_{\mathrm{nanoparticle}} \Big/ S^{\mathrm{2D-IR}}_{\mathrm{isotropic}} \quad (5)$$

$$Q_{\mathrm{IR}} = A^{\mathrm{IR}}_{\mathrm{nanoparticle}} \Big/ A^{\mathrm{IR}}_{\mathrm{isotropic}} \quad (6)$$

For a radial transition dipole distribution at the surface of a spherical metal nanoparticle, the IR absorption and 2D-IR signal strength are therefore enhanced by factors $Q_{\mathrm{IR}} = 9$ and $Q_{\mathrm{2D\text{-}IR}} = 81$, or $Q_{\mathrm{2D\text{-}IR}} = Q_{\mathrm{IR}}{}^2$.

The enhancement factors can be calculated more generally by introducing parameters R and θ_d, the average distance and angle of each dipole with respect to the surface (Figure 1 b). Assuming isotropic averaging around the local azimuthal coordinate ϕ_d, the orientational averages are straightforward to compute numerically (as described in the Supporting Information), and in this manner we find that $Q_{\mathrm{2D\text{-}IR}} = Q_{\mathrm{IR}}{}^2$ is valid for all R and θ_d. Figure 2 shows how Q_{IR} and $Q_{\mathrm{2D\text{-}IR}}$ vary with R and θ_d and that surface enhancement will play a role in the infrared and 2D-IR spectra of spherical nanoparticles for dipole angles up to 70 degrees and distances up to $R \approx a$ from the nanoparticle surface. For values of $\theta_d >$ 70 degrees, Q_{IR} and $Q_{\mathrm{2D\text{-}IR}}$ are actually less than 1. Near-complete suppression of infrared and 2D-IR signals occurs for $\theta_d = 90°$ and $R < a$ (the infrared surface selection rule[16]).

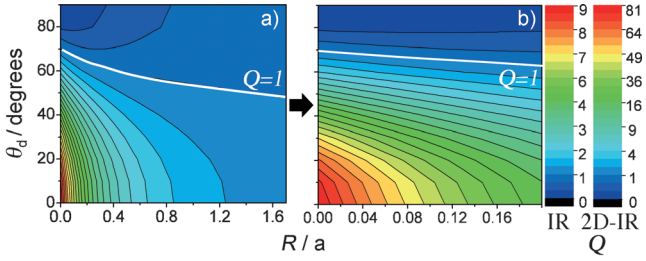

Figure 2. Plots of the IR and 2D-IR signal enhancement factors Q_{IR} and $Q_{\mathrm{2D\text{-}IR}}$ as a function of dipole tilt angle θ_d and distance from the surface R for an orientationally averaged ensemble of dipoles located around a spherical metal nanoparticle of radius a.

To quantify surface enhancement in Raman and IR spectroscopy, it is often necessary to know the molecular surface coverage of the enhancing nanostructure, allowing signal size comparisons to be made against a known concentration of a similar unbound analyte. We can get around this requirement by making use of the fact that 2D-IR signal and infrared absorption are related and both scale linearly with concentration. By measuring 2D-IR signal sizes and infrared absorption strengths from a nanoparticle-bound and a similar unbound "isotropic" species, an experimental measure of enhancement independent of concentration and other instrument parameters is obtained [Eq. (7)]:

$$Q_{\mathrm{exp}} = \frac{S^{\mathrm{2D-IR}}_{\mathrm{nanoparticle}}/A^{\mathrm{IR}}_{\mathrm{nanoparticle}}}{S^{\mathrm{2D-IR}}_{\mathrm{isotropic}}/A^{\mathrm{IR}}_{\mathrm{isotropic}}} = \frac{Q_{\mathrm{2D-IR}}}{Q_{\mathrm{IR}}}\frac{\mu^2_{\mathrm{nanoparticle}}}{\mu^2_{\mathrm{isotropic}}} \quad (7)$$

Equation (7) contains two effects that can change the 2D-IR signal size of the nanoparticle capping layer: the nanoparticle near-field enhancement and the molecular environment change. We assume here that the latter is negligible $\left(\mu^2_{\mathrm{nanoparticle}}\Big/\mu^2_{\mathrm{isotropic}} \approx 1\right)$. Thus, $Q_{\mathrm{2D-IR}}$ is simply $Q_{\mathrm{exp}}{}^2$.

Spherical gold nanoparticles (average radius a of 6.5 and 10 nm) were prepared with amide- and carboxylate-functionalized thiol-based capping molecules attached (Figure 3). The capping molecules and nanoparticles were specifically chosen to simultaneously give stable aqueous suspensions in D_2O and to act as local probes of environment and surface enhancement, providing together a degree of variation in the expected ensemble values of a, R, and θ_d.

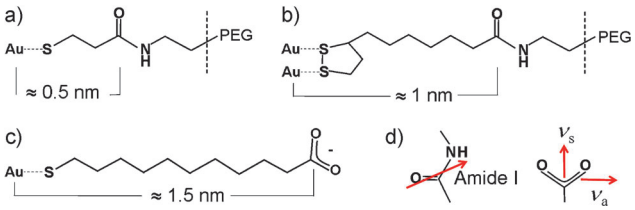

Figure 3. a–c) Nanoparticle capping molecules used herein. The gold-to-reporter distances are for perpendicular alkane spacers. d) Orientation of transition dipole moments of interest.

Molecules (a) and (b) of Figure 3 contain a single amide unit, expected to lie at about 0.5 and 1 nm from the gold "anchor" point, respectively. For these molecules, we studied the amide I band, which has a transition dipole moment pointing approximately 20° away from the carbonyl group towards the nitrogen atom (Figure 3 d).[4d] Molecule (c), mercaptoundecanoic acid (MUA), contains a carboxylate group located about 1.5 nm from the gold anchor point. For this case, we examined the carboxylate symmetric (ν_s) and asymmetric (ν_a) stretch modes (Figure 3 d). The orthogonal transition dipole moments of these modes mean that two (perpendicular) θ_d angles from the same chemical group can be accessed. Lastly, in anticipation of larger field enhancements,[13d] a final parameter that we were able to modify was the nanoparticle morphology itself. Stable submicron-sized

aggregates capped with the 0.5 nm amide-PEG were prepared for analysis alongside the monodisperse spherical nanoparticle samples. The preparation and characterization of all nanoparticle samples and other practical details concerning the 2D-IR spectroscopy are described in the Supporting Information.

Figure 4a and 4b show 2D-IR spectra of the amide I band for the 0.5 nm amide-PEG sample free in solution, and bound to spherical gold nanoparticles. Figure 4c shows a 2D-IR spectrum of nanoparticle-bound 1 nm amide-PEG. Both samples used in Figure 4b and 4c contained nanoparticles with an average radius $a = 6.5$ nm. The FT-IR lineshapes of these three sample types are presented in Figure 4f. The larger radius gold nanoparticles ($a = 10$ nm) and also the aggregated samples tested gave identical infrared and 2D-IR amide I lineshapes. In Figure 4d, 4e, and 4g–i are 2D-IR and FT-IR spectra for MUA-capped nanoparticles. As MUA is insoluble in D_2O, it was necessary to use sodium acetate as the unbound carboxylate reference.

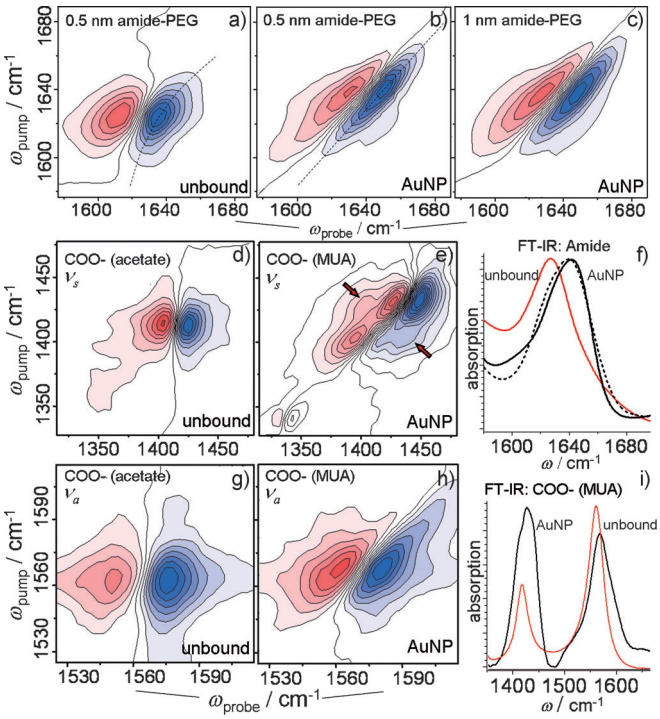

Figure 4. 2D-IR and FT-IR spectra of amide- and carboxyl-reporting groups bound to gold nanoparticles (AuNPs) and in solution (unbound). 2D-IR population time; 300 fs. All samples suspended/dissolved in D_2O/NaOD.

To calculate experimental enhancement values [Q_{exp}, Eq. (7)], the peak values of infrared absorbance and negative diagonal 2D-IR signal (shown in blue in Figure 4) were used for each nanoparticle sample and its unbound reference. Example infrared and 2D-IR datasets for determining Q_{exp} are presented in Figure 5. Here, spectra of the unbound 0.5 nm amide-PEG are shown measured alongside samples of the same capping molecule bound to $a = 6.5$ nm gold nanoparticles and submicron-sized aggregates. The data clearly

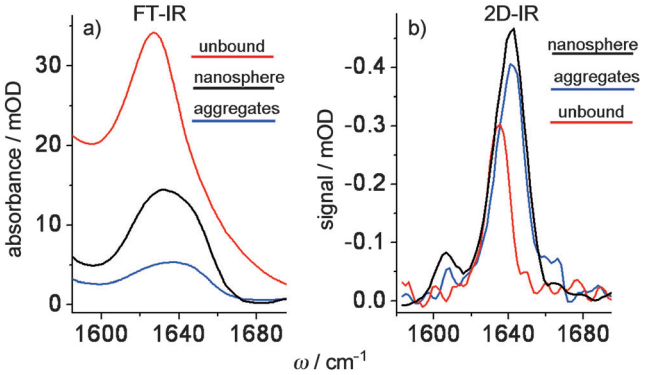

Figure 5. An example dataset for determining experimental enhancement factors (Q_{exp}) from FT-IR absorbance and 2D-IR ground state bleach/stimulated emission spectra of amide I bands. The 2D-IR signal plots are cuts (dotted lines in Figure 5a and 5b) showing the peak values of the negative diagonal signal at each pump frequency.

show that the 0.5 nm amide-PEG 2D-IR signals from nanospheres and aggregates are larger than the 2D-IR signal from the unbound sample, despite the unbound sample having the highest linear absorbance.

The measured enhancement factors Q_{exp} are displayed in Table 1. Values between 2 and 10 are observed, corresponding to 2D-IR signal enhancements of $\times 4$ to $\times 100$ ($Q_{2D\text{-}IR} \cong Q_{exp}^2$).

Table 1: Enhancement measurements on amide- and carboxylate-capped spherical nanoparticles and aggregates.

Sample		$Q_{IR} \pm 20\%$
unbound capping molecule		1
$a = 6.5$ nm AuNPs	1 nm spacer amide I	2
$a = 10$ nm AuNPs	1 nm spacer amide I	2.5
$a = 6.5$ nm AuNPs	0.5 nm spacer amide I	3.5
$a = 10$ nm AuNPs	0.5 nm spacer amide I	4.5
$a = 10$ nm AuNPs, MUA COO- ν_s		5
$a = 10$ nm AuNPs, MUA COO- ν_a		3
aggregated sample, 0.5 nm spacer		10

The Q_{exp} values of the spherical amide-PEG nanoparticles nicely illustrate the effects of changing the dipole distance R and nanoparticle size a. That is, Q_{exp} increases for the samples with the amide group nearer to the surface (the 0.5 nm amide-PEG) and also for the larger diameter nanoparticles. As expected,[13d] increasing the size and degree of disorder of the gold nanostructures by aggregating the nanoparticles causes Q_{exp} for the amide-PEG capping layer to increase to $\times 10$ ($Q_{2D\text{-}IR} = 100$).

We now turn our attention to what the surface-enhanced 2D-IR spectra reveal about the amide-PEG capping layer structure. The rounded 2D lineshape of the unbound amide I band is known to be due to fast dephasing, caused by rapid fluctuations of solvation shell water affecting the hydrogen-bonded amide I′ frequency.[17] In contrast, the nanoparticle-bound amide I 2D spectrum shows a narrower antidiagonal linewidth, demonstrating that as part of a capping layer "core", environmental fluctuations are substantially slower. Despite this difference, the diagonal widths of the bound and

unbound bands are actually similar. The 13.5 cm^{-1} spectral blue-shift observed for amide-PEG upon binding to the nanoparticles is also indicative of a chemical environment change. However, the H_2O-prepared amide-PEG nanoparticles, unlike the unbound amide-PEG molecules do not undergo H-D exchange upon suspension in D_2O.[18] This accounts for about 5 cm^{-1} of the observed 13.5 cm^{-1} blue-shift in the nanoparticle amide I band. The remaining shift is, in a relative sense, rather small and indicates that the carbonyl groups on the nanoparticles are still hydrogen bonded, probably with neighboring amide groups, as has been proposed for similar amide SAMs.[19]

Comparison of the measured enhancement factors for the 0.5 and 1 nm amide-PEG molecules with those calculated in Figure 2 indicate that the amide I transition dipoles are at an average θ_d angle of 45° to 50°, implying that the carbonyl groups are at 65 to 75° relative to the surface normal. This is entirely consistent with the range of angles possible when considering the packing of such capping molecules on a surface.

The MUA-capped nanoparticle 2D-IR spectra offer different, but equally interesting insights. As with the amide I data, the slightly more tilted 2D-IR peaks of the nanoparticle-bound carboxylate groups (compared with the unbound spectrum) suggest slower fluctuations at the surface of the nanoparticle capping layer. This is consistent with previous 2D-IR observations of water near the charged interface of reverse micelles.[20] Comparing the two orthogonal transition dipoles for the MUA capped nanoparticles case (Table 1), we see that the symmetric (ν_s) and asymmetric (ν_a) stretch modes are both enhanced, with the former having a larger value. This implies that both modes have some radial component, with the symmetric stretch mode more axially oriented on the nanoparticle surface. Previous flat gold carboxylate SAM measurements using near-edge EXAFS determined a more "upright" conformation.[21] If this were the case in the 2D-IR spectra of the $a = 10$ nm nanoparticles examined here, the ν_a mode would be suppressed relative to the unbound carboxylate. Nanoparticle curvature effects[22] and compositional differences are the most likely cause of the extra carboxylate tilt compared with the flat surface studies.

Compared with the amide I data presented here, the exact interpretation of the carboxylate enhancements is more nuanced because of the appearance of two diagonal peaks in the symmetric stretch 2D-IR spectrum, separated by about 30 cm^{-1} with cross peaks between them (Figure 5e, red arrows). No such effect is present for the asymmetric stretch mode. This suggests that interactions between carboxylate groups occur upon close packing of the MUA on the nanoparticle surface, resulting in excitonic coupling of the symmetric stretch modes. The carboxylate-capped nanoparticle data is thus an important illustration that through the appearance of cross peaks, 2D-IR spectroscopy can be used to probe associations of molecules in a capping layer.

We note that typical SEIRA applications use rough, percolated and possibly plasmon-resonant surfaces. In comparison, the experiments reported here involve isolated particles and relatively small signal enhancements.[13d] In fact, if the enhancements were larger, we would expect distortions of the 2D-IR lineshapes. Taking the aggregated sample as an example ($Q_{2D\text{-}IR} \approx 100$), based on the number of photons in our pump laser pulse ($\approx 10^{13}$), the estimated number of amide groups in the laser focal volume ($\approx 10^{11}$) and the number of photons absorbed by the pump beam through the about 4 mOD (enhanced) amide I band ($\approx 1\%$ absorbed), we anticipate that any further increase in the near field strength will begin to induce multiphoton processes. These would appear as third (and higher) excited-state absorption bands in the 2D-IR spectrum, stealing intensity from the third order 2D-IR signal.

Although no higher order nonlinear effects appear to be present in the 2D-IR data presented here, these effects should be considered when designing experiments for measuring larger 2D-IR signal enhancements. In this respect, the combination of tip enhancement or infrared plasmonic resonant nanostructured surfaces with low peak intensity, high fluence infrared laser sources[23] appear to be a promising direction.

In summary, we have demonstrated that 2D-IR spectroscopy is a useful method for characterizing the structure and dynamics of nanoparticle capping layers. The measurement strategy presented for detecting the surface enhancement of nanostructure capping layer does not require any knowledge of the capping layer surface coverage. A simple dipole distribution model is used to relate the measured enhancement to the tilt angle and surface distance of the molecular groups probed. Spectra observed from amide and carboxylate groups on spherical and aggregated nanoparticles show that the sensitivity of 2D-IR spectroscopy to surface field enhancements, interaction cross peaks, and different linebroadening mechanisms results in useful structural information that may in future assist in the design and synthesis of novel functionalized nanoparticles. Relating the enhancements, cross peaks, and 2D lineshapes to more realistic capping layer models simulated by, for example, molecular dynamics will be an important step in increasing the available information content.

Received: June 25, 2012
Revised: November 6, 2012
Published online: November 26, 2012

Keywords: IR spectroscopy · laser spectroscopy · nanoparticles · surface analysis · ultrafast dynamics

[1] a) J. C. Love, L. A. Estroff, J. K. Kriebel, R. G. Nuzzo, G. M. Whitesides, *Chem. Rev.* **2005**, *105*, 1103 – 1169; b) M. Brust, M. Walker, D. Bethell, D. J. Schiffrin, R. Whyman, *J. Chem. Soc. Chem. Commun.* **1994**, 801 – 802.

[2] J. F. Li, Y. F. Huang, Y. Ding, Z. L. Yang, S. B. Li, X. S. Zhou, F. R. Fan, W. Zhang, Z. Y. Zhou, D. Y. Wu, B. Ren, Z. L. Wang, Z. Q. Tian, *Nature* **2010**, *464*, 392 – 395.

[3] A. Matschulat, D. Drescher, J. Kneipp, *ACS Nano* **2010**, *4*, 3259 – 3269.

[4] a) W. Zhuang, T. Hayashi, S. Mukamel, *Angew. Chem.* **2009**, *121*, 3804 – 3838; *Angew. Chem. Int. Ed.* **2009**, *48*, 3750 – 3781; b) J. C. Wright, *Annu. Rev. Phys. Chem.* **2011**, *62*, 209 – 230; c) N. T. Hunt, *Chem. Soc. Rev.* **2009**, *38*, 1837 – 1848; d) P. Hamm, M.

Zanni, *Concepts and methods of 2D infrared spectroscopy*, Cambridge University Press, Cambridge, **2010**.
[5] a) P. Hamm, M. H. Lim, R. M. Hochstrasser, *J. Phys. Chem. B* **1998**, *102*, 6123 – 6138; b) M. C. Asplund, M. T. Zanni, R. M. Hochstrasser, *Proc. Natl. Acad. Sci. USA* **2000**, *97*, 8219 – 8224.
[6] a) M. L. Cowan, B. D. Bruner, N. Huse, J. R. Dwyer, B. Chugh, E. T. J. Nibbering, T. Elsaesser, R. J. D. Miller, *Nature* **2005**, *434*, 199 – 202; b) P. Mukherjee, A. T. Krummel, E. C. Fulmer, I. Kass, I. T. Arkin, M. T. Zanni, *J. Chem. Phys.* **2004**, *120*, 10215 – 10224; c) J. N. Bandaria, S. Dutta, S. E. Hill, A. Kohen, C. M. Cheatum, *J. Am. Chem. Soc.* **2008**, *130*, 22 – 23.
[7] a) O. Golonzka, M. Khalil, N. Demirdoven, A. Tokmakoff, *J. Chem. Phys.* **2001**, *115*, 10814 – 10828; b) N. Demirdöven, C. M. Cheatum, H. S. Chung, M. Khalil, J. Knoester, A. Tokmakoff, *J. Am. Chem. Soc.* **2004**, *126*, 7981 – 7990.
[8] D. V. Kurochkin, S. R. G. Naraharisetty, I. V. Rubtsov, *Proc. Natl. Acad. Sci. USA* **2007**, *104*, 14209 – 14214.
[9] a) J. R. Zheng, K. Kwak, J. Asbury, X. Chen, I. R. Piletic, M. D. Fayer, *Science* **2005**, *309*, 1338 – 1343; b) S. Woutersen, Y. Mu, G. Stock, P. Hamm, *Chem. Phys.* **2001**, *266*, 137 – 147.
[10] a) D. E. Rosenfeld, Z. Gengeliczki, B. J. Smith, T. D. P. Stack, M. D. Fayer, *Science* **2011**, *334*, 634 – 639; b) W. Xiong, J. E. Laaser, R. D. Mehlenbacher, M. T. Zanni, *Proc. Natl. Acad. Sci. USA* **2011**, *108*, 20902 – 20907.
[11] H. Bian, J. Li, H. Chen, K. Yuan, X. Wen, Y. Li, Z. Sun, J. Zheng, *J. Phys. Chem. C* **2012**, *116*, 7913 – 7924.
[12] a) D. L. Jeanmaire, R. P. Vanduyne, *J. Electroanal. Chem.* **1977**, *84*, 1 – 20; b) M. Fleischmann, P. J. Hendra, A. J. McQuilla, *Chem. Phys. Lett.* **1974**, *26*, 163 – 166.
[13] a) A. Hartstein, J. R. Kirtley, J. C. Tsang, *Phys. Rev. Lett.* **1980**, *45*, 201 – 204; b) R. Adato, A. A. Yanik, J. J. Amsden, D. L. Kaplan, F. G. Omenetto, M. K. Hong, S. Erramilli, H. Altug, *Proc. Natl. Acad. Sci. USA* **2009**, *106*, 19227 – 19232; c) K. Ataka, J. Heberle, *Anal. Bioanal. Chem.* **2007**, *388*, 47 – 54; d) M. Osawa, M. Ikeda, *J. Phys. Chem.* **1991**, *95*, 9914 – 9919.
[14] C. F. Bohren, D. R. Huffman, *Absorption and scattering of light by small particles*, Wiley-VCH, Weinheim, **1983**.
[15] K. L. Kelly, E. Coronado, L. L. Zhao, G. C. Schatz, *J. Phys. Chem. B* **2003**, *107*, 668 – 677.
[16] R. G. Greenler, D. R. Snider, D. Witt, R. S. Sorbello, *Surf. Sci.* **1982**, *118*, 415 – 428.
[17] M. T. Zanni, M. C. Asplund, R. M. Hochstrasser, *J. Chem. Phys.* **2001**, *114*, 4579 – 4590.
[18] C. Briggs, T. B. Norsten, V. M. Rotello, *Chem. Commun.* **2002**, 1890 – 1891.
[19] R. S. Clegg, J. E. Hutchison, *J. Am. Chem. Soc.* **1999**, *121*, 5319 – 5327; A. K. Boal, V. M. Rotello, *Langmuir* **2000**, *16*, 9527 – 9532.
[20] M. D. Fayer, *Acc. Chem. Res.* **2012**, *45*, 3 – 14.
[21] T. M. Willey, A. L. Vance, T. van Buuren, C. Bostedt, A. J. Nelson, L. J. Terminello, C. S. Fadley, *Langmuir* **2004**, *20*, 2746 – 2752.
[22] H. S. Mandal, H. B. Kraatz, *J. Am. Chem. Soc.* **2007**, *129*, 6356 – 6357.
[23] X. G. Xu, M. Rang, I. M. Craig, M. B. Raschke, *J. Phys. Chem. Lett.* **2012**, *3*, 1836 – 1841.

